

# Improved Catalytic Properties of Pt Cluster Supported on Defective Graphene

Y. Huang<sup>1</sup>, Z. Yu<sup>1</sup>, E. Song<sup>\*2</sup>

<sup>1</sup>School of Science, Nantong University, Nantong 226000, China

<sup>2</sup>State Key Laboratory of High-Performance Ceramics and Superfine Microstructure, Shanghai Institute of Ceramics, Chinese Academy of Sciences, 1295 Dingxi Road, Shanghai 200050, China

received November 3, 2021; received in revised form December 2, 2021; accepted December 8, 2021

## Abstract

Graphene-supported transition-metal nanoparticles demonstrate extraordinary catalytic activity for CO oxidation. Herein, we have applied the density functional theory to investigate the stability and catalytic properties of a Pt<sub>12</sub> cluster adsorbed on a bi-vacancy defective graphene (Pt/graphene). It has been found that the very low energy barrier is only 0.131 eV for the Langmuir-Hinshelwood oxidation process for CO co-adsorbed on a catalyst with an O<sub>2</sub> molecule. The following Eley-Rideal oxidation process is carried out with an activation barrier of 0.352 eV. Furthermore, the bi-vacancy site of graphene plays a key role as an anchoring point for the Pt<sub>12</sub> cluster owing to the strong d-p orbital hybridization, improving the stability and catalytic activity toward CO oxidation. This unusually high catalytic activity opens a new avenue for fabricating carbon-based catalysts for CO oxidation.

*Keywords:* Graphene, Pt cluster, defects

## I. Introduction

Graphene, one planar sheet of sp<sup>2</sup>-bonded carbon atoms arranged in a hexagonal lattice, has recently attracted wide attention in materials science and condensed-matter physics on account of its unique electronic properties<sup>1-3</sup>. Especially, the presence of carbon vacancies on graphene significantly influences its physical and chemical characteristics<sup>4-6</sup>. Graphene vacancies are used as anchoring points for pure metal nanoparticles, ensuring and maximizing the isolated stability and catalytic activity via the availability of uncoordinated surface sites along with a high surface area<sup>7-18</sup>. Thus, modified graphene could increase catalytic efficiency on the basis of interactions between the carbon vacancies and metal clusters.

Platinum clusters are of particular importance as catalysts on account of the changes of mechanical and electronic properties in, for example, the oxygen reduction reaction for fuel cells<sup>10, 12, 19-21</sup>, hydrogenation reactions in organic chemistry<sup>22, 23</sup> and CO oxidation<sup>11, 24-27</sup>. For example, Pt nanoclusters supported on chemically converted graphene exhibit a lower sintering tendency while demonstrating high catalytic activity, which rivals that of state-of-the-art Pt-Ru electrocatalysts<sup>19-21</sup>. Moreover, several research projects have also shown that defects in graphene supports play an important role in stabilizing the catalyst nanoclusters against sintering by providing strong anchoring sites. Besides that, a strong energetic preference for binding Pt clusters at the defect sites in graphene compared to that of pristine graphene sheet has also been theo-

retically verified<sup>28</sup>. This suggests that support defects appreciably regulate the electronic structure of clusters, further improving their catalytic activity<sup>29</sup>.

Herein, we investigate the effects of the bi-vacancy defects in graphene on the catalytic activity of Pt<sub>12</sub> clusters supported on graphene (Pt<sub>12</sub>/graphene). For CO oxidation, it is important to utilize defective-graphene-supported Pt nanoparticles for the enhancement of the catalytic activity of Pt nanoparticles. There are two steps in our research work: (1) Pt<sub>12</sub> nanoparticle adsorption on a bi-vacancy defect site of graphene and (2) CO catalytic oxidation on the Pt<sub>12</sub>-defective graphene. As a result, the Pt<sub>12</sub>/graphene with rich electronic states exhibits a superior performance with an ultralow energy barrier of 0.35 eV for CO oxidation, which is even better than the Pt bulk. Furthermore, this indicates that the presence of the defective graphene substrate enhances the stability of Pt<sub>12</sub>/graphene and improves the catalytic activity.

## II. Computational Method

All density functional theory (DFT) calculations were performed in the Vienna Ab initio simulation package (VASP)<sup>30</sup>. The generalized gradient approximation (GGA) with the Perdew-Burke-Ernzerhof exchange-correlation functional and a 450 eV cutoff for the plane-wave basis set were employed<sup>31</sup>. The projector-augmented plane wave (PAW) was used to describe the electron-ion interactions. A set of (4×4×1) *k*-points were selected for geometric optimization, and the convergence threshold was set as 10<sup>-6</sup> eV in energy and 0.01 eV/Å in force, respectively.

\* Corresponding author: [ehsong@mail.sic.ac.cn](mailto:ehsong@mail.sic.ac.cn)

A hexagonal graphene supercell ( $6 \times 6$  graphene unit cell) containing 70 atoms was introduced to model a system where two C atoms are removed. The modulus unit cell vector in the  $z$  direction was set to 20 Å, which led to negligible interactions between the system and its mirror images. To investigate the minimum energy pathway (MEP) for CO oxidation, linear synchronous transit (LST/QST) and nudged elastic band (NEB)<sup>32</sup> tools were used, which have been well validated to find TS and MEP. The adsorption energy  $E_{ad}$  between the adsorbate and Pt/graphene is defined as:

$$E_{ad} = E_{\text{substrate+adsorbate}} - (E_{\text{substrate}} + E_{\text{adsorbate}}) \quad (1)$$

where the subscripts t, Pt/graphene, and adsorbate denote the total energies, and the energies of the corresponding substances.

### III. Results and Discussion

Fig. 1a shows the schematic geometrical configuration of the Pt<sub>12</sub> cluster adsorbed on graphene (Pt<sub>12</sub>/graphene). In accordance with previous work<sup>33</sup>, we designed the Pt<sub>12</sub> cluster adsorbed on defective graphene. The Pt clusters prefer to sit on a bi-vacancy site to develop bonds with nearby C atoms of graphene. The lattice mismatch between Pt atoms that are directly bonded to the C atoms is elongated by 0.13 Å, which may contribute to its stability, as in the case of the defective-graphene-enhanced stability of metal nanoclusters<sup>12, 25, 34–36</sup>. The average bond length between the neighboring Pt and C ( $l_{\text{Pt-C}}$ ) is about 2.218 Å, and the distance between the Pt<sub>12</sub> cluster and the graphene sheet is around 2.233 Å. Meanwhile, there is about 0.369 $e$  charge transfer ( $Q$ ) from the Pt<sub>12</sub> cluster to the defective graphene sheet according to Hirshfeld charge population analysis, and the adsorption energy of Pt<sub>12</sub> cluster is 3.293 eV. Obviously, different electron affinities of Pt<sub>12</sub> cluster and C change the electron distribution of

the Pt<sub>12</sub>/graphene system. Therefore, we show that the carbon vacancies or dangling bonds of carbon atoms significantly enhance the stability of Pt<sub>12</sub> clusters on defective graphene, and regulate the electronic structure of Pt<sub>12</sub> clusters.

To gain a deeper insight into the electron structure of Pt<sub>12</sub>/graphene, the partial density of states projected on Pt-5 $d$  and Pt-6 $s$  orbitals and neighboring C-2 $p$  orbital is plotted, as shown in Fig. 1d. Owing to the formation of C-Pt bonds and charge transfer from Pt to C, Pt-6 $s$ , Pt-5 $d$ , and C-2 $p$  orbitals are strongly hybridized at around deep level  $-4 \sim -6$  eV. In addition, the high density of states is localized around  $E_F$  while the localized Pt-5 $d$  orbital is important to activate reactants to lower the CO oxidation barriers.

Herein, we first consider the adsorptions of CO and O<sub>2</sub> with Pt<sub>12</sub>/graphene, respectively. Fig. 1b shows the most stable end-on configuration of CO on Pt<sub>12</sub>/graphene system with  $E_{ad}(\text{CO}) = -2.857$  eV. Meanwhile, there is about 0.075 $e$  charge transfer from Pt<sub>12</sub>/graphene to CO, which subsequently leads to the elongation of  $l_{\text{C-O}}$  from 1.131 to 1.172 Å. As shown in Fig. 1e, strong hybridization between Pt-5 $d$  and CO-2 $p$  orbitals is observed at around  $-4 \sim -2$  eV from the computed PDOS. This indicates that the variation in bond strength is caused by CO 2 $p$  and Pt-5 $d$  coupling; namely, the stronger this coupling is, the stronger the CO-metal bonding is<sup>37</sup>.

In Fig. 1c, for O<sub>2</sub> adsorption on Pt<sub>12</sub>/graphene, the most energetically favorable configuration is parallel to the graphene sheet forming the chemical bond with the Pt (top site) where  $E_{ad}(\text{O}_2) = -1.061$  eV, which is also favorable compared to the end-on configuration of CO. Meanwhile, there is about 0.197 $e$  charge transfer from Pt<sub>12</sub>/graphene to O<sub>2</sub>, elongating  $l_{\text{O1-O2}}$  from 1.213 to 1.287 Å. For this case, the apparently strong hybridization between Pt-5 $d$  and O<sub>2</sub>-2 $p$  orbitals is observed at around  $-2 \sim 0$  eV (Fig. 1f).

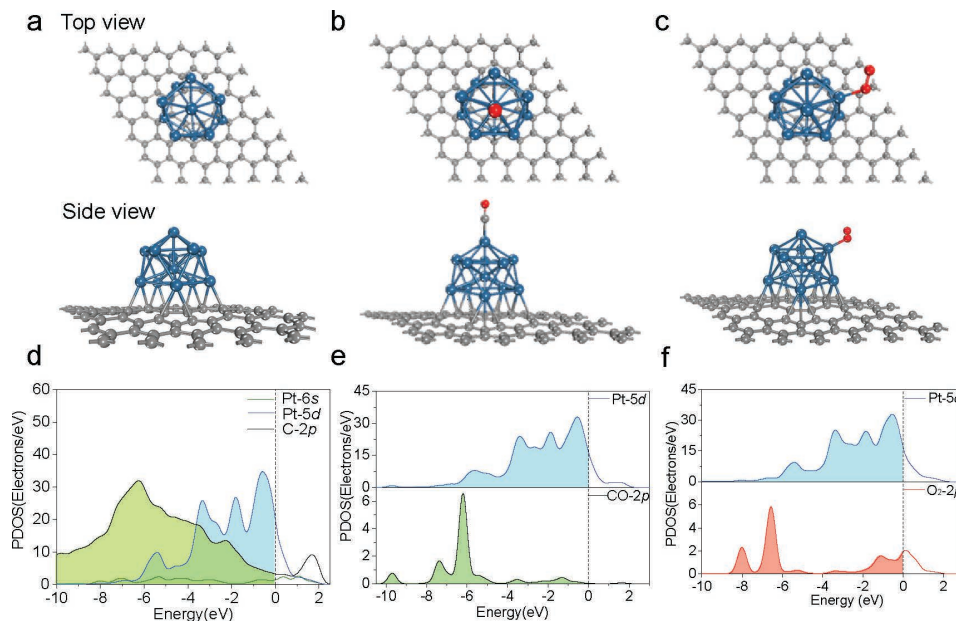


**Fig. 1:** Top and side views of the geometric (a-c) and electronic (d-f) structures of Pt/graphene, CO on Pt/graphene and O<sub>2</sub> on Pt/graphene. The blue, small gray and red ball represents the Pt, carbon and oxygen atoms, respectively. (c) Spin-polarized local density of states projected on Pt-5 $d$  (red), Pt-6 $s$  (blue) and CO-2 $p$  (black for neighboring carbon atoms) orbital curves. The Fermi level is set to zero.

Owing to the CO interacting with the Pt<sub>12</sub>/graphene much more strongly than O<sub>2</sub>, the Pt<sub>12</sub> cluster on graphene prefers to be covered by the CO molecule when CO and O<sub>2</sub> are co-adsorbed, which is also an exothermic process with  $E_{\text{ad}}(\text{CO}+\text{O}_2) = -3.647$  eV, being larger than  $E_{\text{ad}}(\text{CO})$  and  $E_{\text{ad}}(\text{O}_2)$ . Actually, the stronger bonding strength between the adsorbates and the catalyst efficiently facilitates associated product formation<sup>38,39</sup>. In addition, there is about 0.230e charge transfer ( $Q$ ) from the Pt<sub>12</sub>/graphene sheet to the CO+O<sub>2</sub>. Besides, the most stable adsorption site of CO<sub>2</sub> on Pt<sub>12</sub> (end-on configuration) with  $E_{\text{ad}}(\text{CO}_2) = -0.143$  eV based on screening of various possible adsorption sites, which reveal a weak adsorption of CO<sub>2</sub> and can easily be desorbed from Pt<sub>12</sub>/graphene.

For CO oxidation, there are two well-established reaction mechanisms [Langmuir-Hinshelwood (LH) and Eley-Rideal (ER)] between adsorbed CO and O<sub>2</sub><sup>26,34,38-44</sup>. Based on the above discussion, it has been shown that both the O<sub>2</sub> molecule and CO molecule could efficiently adsorb on the Pt<sub>12</sub> cluster anchored on graphene. Considering the fact that the bonding energy for CO adsorption is stronger while it is relatively weak for O<sub>2</sub> adsorption, the co-adsorption configuration of CO and O as for the initial states could be feasible. Thus, LH reaction of  $\text{CO} + \text{O}_2 \rightarrow \text{OOCO} \rightarrow \text{CO}_2 + \text{O}$  as an initial state, ER reaction of  $\text{CO} + \text{O} \rightarrow \text{CO}_2$  is followed. In order to search for the minimum-energy pathway (MEP), we further screened the most stable co-adsorption configuration as an initial state (IS1), where CO and O<sub>2</sub> are nearly perpendicular to the graphene sheet, respectively (Fig. 2a). Especially, the final state (FS) consists of a CO<sub>2</sub> molecule physisorbed on Pt<sub>12</sub>/graphene with a chemisorbed atomic O nearby (Fig. 2c). In addition, the local configurations of the reactants on Pt<sub>12</sub>/graphene at each state along MEP are also shown in Fig. 3.

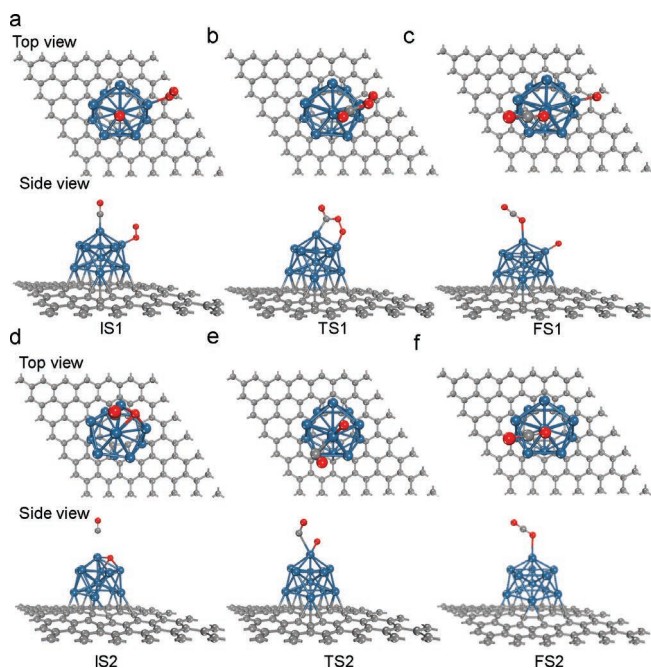


**Fig. 2:** Top and side views of the geometric structures of the initial state (IS1), transition state (TS1), final state (FS1), initial state (IS2), transition state (TS2) and final state (FS2) at each state along MEP.

As shown in Fig. 3, this reveals the minimum energy path obtained with the NEB method for the co-adsorption configuration. The Langmuir-Hinshelwood (LH) oxidation process<sup>9,26,34,44</sup> preferably proceeds with a small activation energy of 0.131 eV (Fig. 3a). The structure of the initial co-adsorption configuration (IS1) would form the close co-adsorption configuration, the elongation of O1-O<sub>2</sub> bond length (transition state TS1), and the formation of a CO<sub>2</sub> molecule via combining the CO molecule with an O atom (FS1), and finally the movement of the single O atom to its best adsorption site on Pt cage (Fig. 2a-c). Once CO and O<sub>2</sub> are co-adsorbed on Pt<sub>12</sub>/graphene, one oxygen atom O approaches C of CO and reaches TS1. The energy barrier  $E_r$  along MEP is estimated to be 0.131 eV. Meanwhile, a peroxy-type O1-O<sub>2</sub>-C-O complex is formed above the Pt<sub>12</sub> cluster. There is about 0.380e charge transfer from the Pt<sub>12</sub>/graphene sheet to the O-O-C-O complex. The bond length  $l_{\text{O-O}}$  increases from 1.287 to 1.540 Å in this exothermic process. The reaction continuously proceeds from TS1 to FS1 where CO<sub>2</sub> is formed, leaving an atomic O1 adsorbed on the Pt<sub>12</sub>/graphene. There is about 0.204e charge transfer from the Pt<sub>12</sub>/graphene sheet to the O1 (-0.283e) and CO<sub>2</sub> (0.079e). Thus, the Pt clusters on graphene contribute to catalyzing the CO oxidation. The preadsorbed elongated pre-oxygen molecule could be activated by a low energy barrier to decompose and offer oxygen atoms for the CO oxidation. The CO<sub>2</sub> is quite inert and prefers to desorb from the Pt<sub>12</sub>/graphene system owing to the weak adsorption. An oxygen atom adsorbed on the anchored Pt cluster, the byproduct material of the LH oxidation, would prepare to oxidize a succeeding CO molecule.

As shown in Fig. 2d-f, the Eley-Rideal (ER) reaction could proceed after the LH reaction. As shown in Fig. 2d, the CO molecule approaching the preadsorbed O atom from the faraway site (IS2) would form the chemical adsorption configuration (transition state TS2), then develop a bond with the O atom to form a CO<sub>2</sub> molecule (FS2). The ER reaction can be driven by activation energy as low as 0.352 eV, which can be easily overcome in the reaction process. It could be concluded that the CO and O<sub>2</sub> co-adsorption configuration controls the oxidation with a small perturbation to start the LH reaction, followed by the ER reaction to reach the final production of an intact anchored Pt cluster on graphene, realizing the catalytic CO oxidation circulation. Thus, CO<sub>2</sub> can be easily desorbed from the Pt/graphene system owing to the weak adsorption. In a comparison with several previous works<sup>45-47</sup>, it has been found that the largest  $E_r = 0.353$  eV is much lower than that of commonly used catalysts such as Pt<sup>48-56</sup>, Pd<sup>52,54-59</sup>, Rh<sup>52,54-56,60-63</sup>, Au<sup>64-68</sup>, etc., merely around 1.00 eV. Note that the values for Au/graphene and Fe/graphene systems are 0.31 eV and 0.58 eV<sup>38,39</sup>.

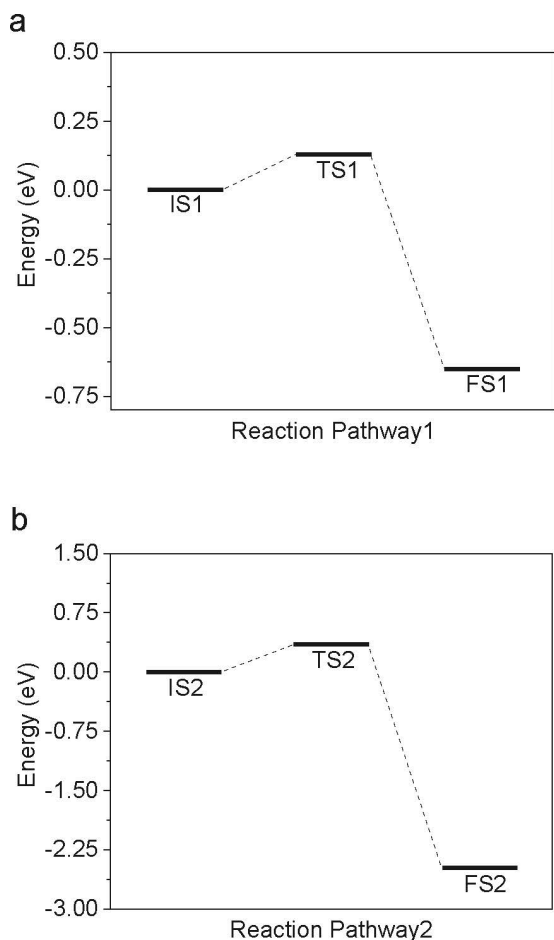


**Fig. 3:** Schematic energy profile corresponding to local configurations of the adsorbates on Pt/graphene at each state along the minimum-energy pathway (MEP). In the first step, corresponding structures include IS1 (a), TS1(b) and FS1(c) along MEP via  $\text{CO} + \text{O}_2 \rightarrow \text{OOCO} \rightarrow \text{CO}_2 + \text{O}$  route. (e-h) In the second step, corresponding final structures include O atom on Pt/graphene (e), IS2 (d), TS2(e) and FS2(f) for  $\text{CO}_2$  formed on Pt/graphene via  $\text{CO} + \text{O} \rightarrow \text{CO}_2$  route. All energies are given in respect of the reference energy.

To gain more insight into the origin of the high activity of the Pt/graphene system, we have investigated the electron-

ic structures as the LH reaction progresses. As discussed above, the partially occupied Pt-5d orbital, being crucial for the activity, is localized around  $E_F$  owing to the interaction between the Pt<sub>12</sub> and graphene. Fig. 4 shows the electronic local density of states (LDOS) projected onto the C-O and O-O bonds, as well as the *d*-projected LDOS of Pt in IS, TS1 and FS1 of the LH step, respectively. The *s*- and *p*-projected LDOS of Pt<sub>12</sub> and *p*-projected LDOS of C have no significant change as the reaction progresses and are thus not shown here. Upon CO and O<sub>2</sub> co-adsorption, Pt<sub>12</sub>-5d orbital is partially occupied in IS1 configuration with the charge transfer between Pt and adsorbates. Owing to the strong hybridization with Pt-5d orbital, the chemical bond between CO and O<sub>2</sub> is formed. In Fig. 2b (TS1), the 2p orbital of CO and O<sub>2</sub> is broadened and more involved with Pt-5d orbital, compared with Fig. 2a, which contributes to weakening the O-O bond. From TS1 to FS1, this indicates that the 2p orbital of CO<sub>2</sub> is weakly hybridized with Pt-5d orbital around -6~-4 eV owing to the physical interaction between the CO<sub>2</sub> and Pt<sub>12</sub>/graphene. For comparison, the O-2p orbitals have strong hybridization with Pt-5d orbital near the  $E_F$  (-2~0 eV). In Fig. 4d, for the C-O species on Pt/graphene, the CO-2p orbital is weakly hybridized with Pt-5d orbital due to the far distance from the Pt cluster. From IS2 to TS2, the CO-2p orbital is gradually strongly hybridized with Pt-5d orbital, leading to the decrease of the bond from the O atom and CO (TS2), finally forming the O-C-O bond length close to the value of  $l_{\text{C-O}}$  of an isolated CO<sub>2</sub> molecule. Thus, Pt-5d orbital dominates the interaction between CO and O<sub>2</sub> on the Pt/graphene system.

In light of the above discussion, we conclude that CO oxidation on Pt/graphene may be characterized as a two-step process: LH reaction initiates CO oxidation with  $E_r = 0.131$  eV, followed by the ER reaction with  $E_r = 0.352$  eV energy barrier. The two reaction steps could proceed rapidly because of the low  $E_r$  values involved.

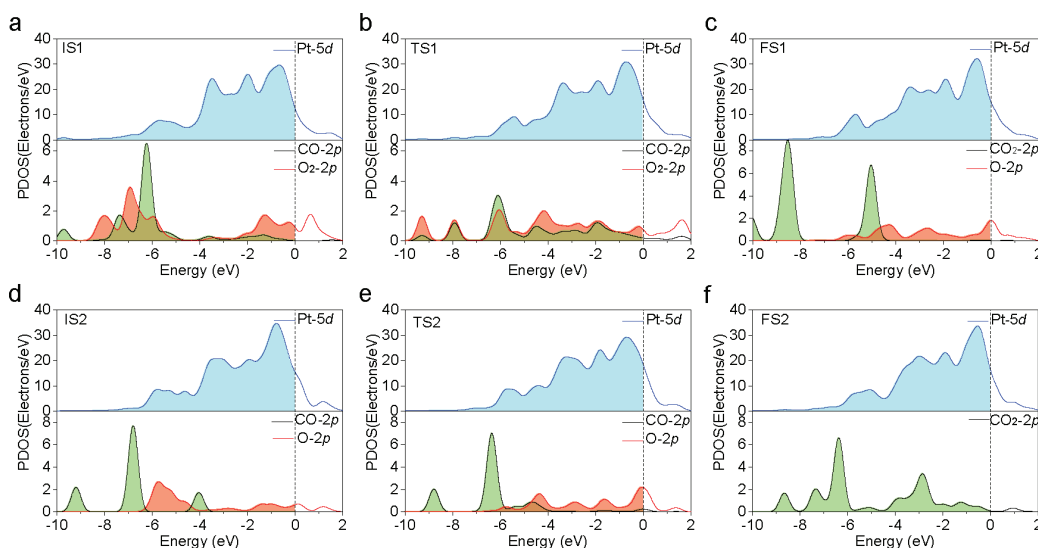


**Fig. 4:** Spin-polarized local density of states (LDOS) projected onto CO+O<sub>2</sub>, OOCO, CO<sub>2</sub>+O on the Pt/graphene (Fig. 2a-c), together with the CO+O, OC-O, CO<sub>2</sub> on the O-Pt/graphene (Fig. 2d-f). Black solid curve, C-O on Cu/graphene; blue soled curve, O1-O2 on Pt/graphene; red curve, *d*-projected LDOS of the Pt atom. The Fermi level is set to zero. .

#### IV. Conclusions

In summary, we performed DFT calculations to investigate the reaction mechanism of CO oxidation catalyzed by a Pt<sub>12</sub>/graphene system, as well as structural and electronic properties of adsorbates and adsorbents. It has been found that the system demonstrates high catalytic activity via the oxidation reaction of the CO molecule. CO oxidation most likely proceeds with an LH reaction as the starting point with lower activation barriers of 0.131 eV, followed by an ER reaction with 0.352 eV energy barrier. The high activity of Pt<sub>12</sub>/graphene may be attributed to the electronic resonance among electronic states of CO, O<sub>2</sub>, and the Pt atom, particularly, among Pt-5*d*, CO-2*p* and O<sub>2</sub>-2*p* orbitals. This good catalytic activity shows that the Pt<sub>12</sub>/graphene system is a good candidate for CO oxidation on account of its higher activity.

#### Acknowledgements

We acknowledge support by the National Natural Science Foundation of China (11604163) and Science and Technology Commission of Shanghai Municipality (21ZR1472900).

#### References

- Geim, A.K.: Graphene: status and prospects, *Science*, **324**, 1530–1534, (2009).
- Allen, M.J., Tung, V.C., Kaner, R.B.: Honeycomb Carbon: A review of graphene, *Chem. Rev.*, **110**, 132–145, (2010).
- Zhuo, H.-Y., Zhang, X., Liang, J.-X., Yu, Q., Xiao, H., Li, J.: Theoretical understandings of Graphene-based metal single-atom Catalysts: stability and catalytic performance, *Chem. Rev.*, **120**, 12315–12341, (2020).
- Singh, A.K., Penev, E.S., Yakobson, B.I.: Vacancy clusters in graphene as quantum dots, *ACS Nano*, **4**, 3510–3514, (2010).
- Boukhalvalov, D.W., Katsnelson, M.I.: Chemical functionalization of graphene with defects, *Nano Lett.*, **8**, 4373–4379, (2008).
- Fan, Y., Song, E., Mustafa, T., Liu, R., Qiu, P., Zhou, W., Zhou, Z., Kawasaki, A., Shirasu, K., Hashida, T., Liu, J., Wang, L., Jiang, W., Luo, W.: Liquid-phase assisted engineering of highly strong SiC composite reinforced by multiwalled carbon nanotubes, *Adv. Sci.*, **7**, 2002225, (2020).
- Kim, G., Jhi, S.-H.: Carbon monoxide-tolerant platinum nanoparticle catalysts on defect-engineered graphene, *ACS Nano*, **5**, 805–810, (2011).
- Krasheninnikov, A.V., Lehtinen, P.O., Foster, A.S., Pyykko, P., Nieminen, R.M.: Embedding transition-metal atoms in Graphene: structure, bonding, and magnetism, *Phys. Rev. Lett.*, **102**, 126807, (2009).
- Song, E.H., Wen, Z., Jiang, Q.: CO catalytic oxidation on copper-embedded graphene, *J. Phys. Chem. C*, **115**, 3678–3683, (2011).
- Yoo, E., Okada, T., Akita, T., Kohyama, M., Nakamura, J., Honma, I.: Enhanced electrocatalytic activity of Pt nanoclusters on graphene nanosheet surface, *Nano Lett.*, **9**, 2255–2259, (2009).
- Zhang, H., Jin, M., Liu, H., Wang, J., Kim, M.J., Yang, D., Xie, Z., Liu, J., Xia, Y.: Facile synthesis of Pd-Pt alloy nanocages and their enhanced performance for preferential oxidation of CO in excess hydrogen, *ACS Nano*, **5**, 8212–8222, (2011).
- Lim, D.-H., Wilcox, J.: Mechanisms of the oxygen reduction reaction on defective graphene-supported Pt nanoparticles from first-principles, *J. Phys. Chem. C*, **116**, 3653–3660, (2012).
- Liu, X., Li, L., Meng, C., Han, Y.: Palladium Nanoparticles/Defective graphene composites as oxygen reduction Electrocatalysts: A first-principles study, *J. Phys. Chem. C*, **116**, 2710–2719, (2011).
- Zhang, L., Si, R., Liu, H., Chen, N., Wang, Q., Adair, K., Wang, Z., Chen, J., Song, Z., Li, J., Banis, M. N., Li, R., Sham, T.-K., Gu, M., Liu, L.-M., Botton, G.A., Sun, X.: Atomic layer deposited Pt-Ru dual-metal dimers and identifying their active sites for hydrogen evolution reaction, *Nat. Commun.*, **10**, 4936, (2019).
- Song, E.H., Yan, J.M., Lian, J.S., Jiang, Q.: External electric field catalyzed N<sub>2</sub>O decomposition on Mn-embedded graphene, *J. Phys. Chem. C*, **116**, 20342–20348, (2012).
- Xiao, B.B., Yang, L., Liu, H.Y., Jiang, X.B., Aleksandr, B., Song, E.H., Jiang, Q.: Designing fluorographene with FeN<sub>4</sub> and CoN<sub>4</sub> moieties for oxygen electrode reaction: A density functional theory study, *Appl. Surf. Sci.*, **537**, 147846, (2021).
- Hu, C., Song, E., Wang, M., Chen, W., Huang, F., Feng, Z., Liu, J., Wang, J.: Partial-Single-atom, partial-nanoparticle composites enhance water dissociation for hydrogen evolution, *Adv. Sci.*, **8**, 2001881, (2021).
- Zhou, Y., Song, E., Chen, W., Segre, C.U., Zhou, J., Lin, Y.-C., Zhu, C., Ma, R., Liu, P., Chu, S., Thomas, T., Yang, M., Liu, Q., Suenaga, K., Liu, Z., Liu, J., Wang, J.: Dual-metal interbonding as the chemical facilitator for single-atom dispersions, *Adv. Mater.*, **32**, 2003484, (2020).
- Guo, S., Sun, S.: FePt nanoparticles assembled on graphene as enhanced catalyst for oxygen reduction reaction, *J. Am. Chem. Soc.*, **134**, 2492–2495, (2012).
- Toyoda, E., Jinnouchi, R., Hatanaka, T., Morimoto, Y., Mitsuhara, K., Visikovskiy, A., Kido, Y.: The d-band structure of Pt nanoclusters correlated with the catalytic activity for an oxygen reduction reaction, *J. Phys. Chem. C*, **115**, 21236–21240, (2011).
- Nethravathi, C., Anumol, E.A., Rajamathi, M., Ravishankar, N.: Highly dispersed ultrafine Pt and PtRu nanoparticles on graphene: formation mechanism and electrocatalytic activity, *Nanoscale*, **3**, 569, (2011).
- Crampton, A.S., Rötzer, M.D., Ridge, C.J., Schweinberger, F.F., Heiz, U., Yoon, B., Landman, U.: Structure sensitivity in the non-scalable regime explored via catalysed ethylene hydrogenation on supported platinum nanoclusters, *Nat. Commun.*, **7**, 10389, (2016).
- Bratlie, K.M., Lee, H., Komvopoulos, K., Yang, P., Somorjai, G.A.: Platinum nanoparticle shape effects on benzene hydrogenation selectivity, *Nano Lett.*, **7**, 3097–3101, (2007).
- Yoo, E., Okada, T., Akita, T., Kohyama, M., Honma, I., Nakamura, J.: Sub-nano-Pt cluster supported on graphene nanosheets for CO tolerant catalysts in polymer electrolyte fuel cells, *J. Power Sources*, **196**, 110–115, (2011).
- Lim, D.-H., Wilcox, J.: DFT-based study on oxygen adsorption on defective graphene-supported Pt nanoparticles, *J. Phys. Chem. C*, **115**, 22742–22747, (2011).
- Zhou, M., Zhang, A., Dai, Z., Zhang, C., Feng, Y.P.: Greatly enhanced adsorption and catalytic activity of Au and Pt clusters on defective graphene, *J. Chem. Phys.*, **132**, 194704, (2010).
- Qin, W., Li, X.: A theoretical study on the catalytic synergistic effects of Pt/Graphene nanocomposites, *J. Phys. Chem. C*, **114**, 19009–19015, (2010).
- Vedala, H., Sorescu, D.C., Kotchey, G.P., Star, A.: Chemical sensitivity of graphene edges decorated with metal nanoparticles, *Nano Lett.*, **11**, 2342–2347, (2011).
- Kou, R., Shao, Y., Mei, D., Nie, Z., Wang, D., Wang, C., Viswanathan, V.V., Park, S., Aksay, I.A., Lin, Y., Wang, Y., Liu, J.: Stabilization of electrocatalytic metal nanoparticles at metal-metal oxide-graphene triple junction points, *J. Am. Chem. Soc.*, **133**, 2541–2547, (2011).

- 30 Kresse, G., Furthmüller, J.: Efficient iterative schemes for ab initio total-energy calculations using a plane-wave basis set, *Phys. Rev. B*, **54**, 11169–11186, (1996).
- 31 Blöchl, P.E.: Projector augmented-wave method, *Phys. Rev. B*, **50**, 17953–17979, (1994).
- 32 Henkelman, G., Jonsson, H.: Improved tangent estimate in the nudged elastic band method for finding minimum energy paths and saddle points, *J. Chem. Phys.*, **113**, 9978–9985, (2000).
- 33 Gao, W., Mueller, J.E., Anton, J., Jiang, Q., Jacob, T.: Nickel cluster growth on defect sites of Graphene: A computational study, *Angew. Chem. Int. Edit.*, **52**, 14237–14241, (2013).
- 34 Chen, G., Li, S.J., Su, Y., Wang, V., Mizuseki, H., Kawazoe, Y.: Improved stability and catalytic properties of Au<sub>16</sub> cluster supported on graphane, *J. Phys. Chem. C*, **115**, 20168–20174, (2011).
- 35 Fampiou, I., Ramasubramaniam, A.: Binding of Pt nanoclusters to point defects in Graphene: adsorption, morphology, and electronic structure, *J. Phys. Chem. C*, **116**, 6543–6555.
- 36 Lim, D.-H., Negreira, A.S., Wilcox, J.: DFT studies on the interaction of defective graphene-supported Fe and Al nanoparticles, *J. Phys. Chem. C*, **115**, 8961–8970, (2011).
- 37 Crawford, P., Hu, P.: Importance of electronegativity differences and surface structure in molecular dissociation reactions at transition metal surfaces, *J. Phys. Chem.*, **110**, 24929–24935, (2006).
- 38 Lu, Y.H., Zhou, M., Zhang, C., Feng, Y.P.: Metal-embedded Graphene: A possible catalyst with high activity, *J. Phys. Chem. C*, **113**, 20156–20160, (2009).
- 39 Li, Y., Zhou, Z., Yu, G., Chen, W., Chen, Z.: CO catalytic oxidation on iron-embedded graphene: Computational quest for low-cost nanocatalysts, *J. Phys. Chem.*, **114**, 6250–6254, (2010).
- 40 An, W., Pei, Y., Zeng, X.C.: CO oxidation catalyzed by single-walled helical gold nanotube, *Nano Lett.*, **8**, 195–202, (2008).
- 41 Molina, L.M., Hammer, B.: The activity of the tetrahedral Au<sub>20</sub> cluster: charging and impurity effects, *J. Catal.*, **233**, 399–404, (2005).
- 42 Tang, D., Hu, C.: DFT insight into CO oxidation catalyzed by gold Nanoclusters: charge effect and multi-state reactivity, *J. Phys. Chem. Lett.*, **2**, 2972–2977, (2011).
- 43 Li, F., Zhao, J., Chen, Z.: Fe-anchored graphene Oxide: A low-cost and easily accessible catalyst for low-temperature CO oxidation, *J. Phys. Chem. C*, **116**, 2507–2514, (2012).
- 44 Zhou, M., Zhang, A., Dai, Z., Feng, Y.P., Zhang, C.: Strain-enhanced stabilization and catalytic activity of metal nanoclusters on graphene, *J. Phys. Chem. C*, **114**, 16541–16546, (2010).
- 45 Jiang, Q., Zhang, J., Ao, Z., Huang, H., He, H., Wu, Y.: First principles study on the CO oxidation on Mn-embedded divacancy graphene, *Front. Chem.*, **6**, (2018).
- 46 Jiang, Q., Huang, M., Qian, Y., Miao, Y., Ao, Z.: Excellent sulfur and water resistance for CO oxidation on Pt single-atom-catalyst supported by defective graphene: the effect of vacancy type, *Appl. Surf. Sci.*, **566**, 150624, (2021).
- 47 Jiang, Q., Zhang, J., Huang, H., Wu, Y., Ao, Z.: A novel single-atom catalyst for CO oxidation in humid environmental conditions: Ni-embedded divacancy graphene, *J. Mater. Chem. A*, **8**, 287–295, (2020).
- 48 Ackermann, M.D., Pedersen, T.M., Hendriksen, B.L.M., Robach, O., Bobaru, S.C., Popa, I., Quiros, C., Kim, H., Hammer, B., Ferrer, S., Frenken, J.W.M.: Structure and reactivity of surface oxides on Pt(110) during catalytic CO oxidation, *Phys. Rev. Lett.*, **95**, 255505, (2005).
- 49 Nakai, I., Kondoh, H., Amemiya, K., Nagasaka, M., Nambu, A., Shimada, T., Ohta, T.: Reaction-path switching induced by spatial-distribution change of reactants: CO oxidation on Pt(111), *J. Chem. Phys.*, **121**, 5035–5038, (2004).
- 50 Alavi, A., Hu, P., Deutsch, T., Silvestrelli, P.L., Hutter, J.: CO oxidation on Pt(111): An ab initio density functional theory study, *Phys. Rev. Lett.*, **80**, 3650, (1998).
- 51 Eichler, A., Hafner, J., Reaction channels for the catalytic oxidation of CO on Pt(111), *Surf. Sci.*, **435**, 58–62, (1999).
- 52 Eichler, A.: CO oxidation on transition metal surfaces: Reaction rates from first principles, *Surf. Sci.*, **498**, 314–320, (2002).
- 53 Bleakley, K., Hu, P.: A density functional theory study of the interaction between CO and O on a Pt Surface: CO/Pt(111), O/Pt(111), and CO/O/Pt(111), *J. Am. Chem. Soc.*, **121**, 7644–7652, (1999).
- 54 Chen, M.S., Cai, Y., Yan, Z., Gath, K.K., Axnanda, S., Goodman, D.W.: Highly active surfaces for CO oxidation on Rh, Pd, and Pt, *Surf. Sci.*, **601**, 5326–5331, (2007).
- 55 Oh, S.-H., Hoflund, G.B.: Low-temperature catalytic carbon monoxide oxidation over hydrous and anhydrous palladium oxide powders, *J. Catal.*, **245**, 35–44, (2007).
- 56 Liu, W., Zhu, Y.F., Lian, J.S., Jiang, Q.: Adsorption of CO on surfaces of 4d and 5d elements in group VIII, *J. Phys. Chem. C*, **111**, 1005–1009, (2006).
- 57 Nakai, I., Kondoh, H., Shimada, T., Resta, A., Andersen, J.N., Ohta, T.: Mechanism of CO oxidation reaction on O-covered Pd(111) surfaces studied with fast X-ray photoelectron spectroscopy: change of reaction path accompanying phase transition of O domains, *J. Chem. Phys.*, **124**, 224712, (2006).
- 58 Zhang, C.J., Hu, P.: CO oxidation on Pd(100) and Pd(111): A comparative study of reaction pathways and reactivity at low and medium coverages, *J. Am. Chem. Soc.*, **123**, 1166–1172, (2001).
- 59 Salo, P., Honkala, K., Alatalo, M., Laasonen, K.: Catalytic oxidation of CO on Pd(111), *Surf. Sci.*, **516**, 247–253, (2002).
- 60 Krenn, G., Bako, I., Schennach, R.: CO adsorption and CO and O coadsorption on Rh(111) studied by reflection absorption infrared spectroscopy and density functional theory, *J. Chem. Phys.*, **124**, 144703, (2006).
- 61 Slijivancanin, Z., Hammer, B.: CO oxidation on fully oxygen covered Ru(0001): role of step edges, *Phys. Rev. B*, **81**, 121413, (2010).
- 62 Liu, D.J.: CO oxidation on Rh(100): multisite atomistic lattice-gas modeling, *J. Phys. Chem. C*, **111**, 14698–14706, (2007).
- 63 Stampfl, C., Scheffler, M.: Density-functional theory study of the catalytic oxidation of CO over transition metal surfaces, *Surf. Sci.*, **433**, 119–126, (1999).
- 64 Kimble, M.L., Castleman, A.W., Mitrić, R., Bürgel, C., Bonačić-Koutecký, V.: Reactivity of atomic gold anions toward oxygen and the oxidation of CO: Experiment and theory, *J. Am. Chem. Soc.*, **126**, 2526–2535, (2004).
- 65 Socaciu, L.D., Hagen, J., Bernhardt, T.M., Wöste, L., Heiz, U., Häkkinen, H., Landman, U.: Catalytic CO oxidation by free Au<sub>2</sub>⁻: experiment and theory, *J. Am. Chem. Soc.*, **125**, 10437–10445, (2003).
- 66 Lopez, N., Nørskov, J.K.: Catalytic CO oxidation by a gold Nanoparticle: A density functional study, *J. Am. Chem. Soc.*, **124**, 11262–11263, (2002).
- 67 Liu, Z.P., Hu, P., Alavi, A.: Catalytic role of gold in gold-based catalysts: A density functional theory study on the CO oxidation on gold, *J. Am. Chem. Soc.*, **124**, 14770–14779, (2002).
- 68 Kandoi, S., Gokhale, A.A., Grabow, L.C., Dumesic, J.A., Mavrikakis, M.: Why Au and Cu are more selective than Pt for preferential oxidation of CO at low temperature, *Catal. Lett.*, **93**, 93–100, (2004).